

Line Stretching in Random Flows

D. R. Lester

*School of Engineering, RMIT University, 3000 Melbourne, Australia**

M. Dentz

Spanish National Research Council (IDAEA-CSIC), 08034 Barcelona, Spain

(Dated: April 28, 2025)

An *ab initio* analysis of stretching of the length $l(t)$ of material lines in steady and unsteady random chaotic flows is performed under Fickian and non-Fickian (anomalous) transport. We show that fluid stretching is an autocatalytic process with finite sampling that is governed by a competition between ensemble and temporal averaging processes. The topological entropy $h \equiv \lim_{t \rightarrow \infty} \ln l(t)/t$ converges to the Lyapunov exponent λ_∞ in Fickian flows, whereas in non-Fickian flows h converges to λ_∞ plus a contribution from the variance σ_λ^2 of the finite time Lyapunov exponent. This study uncovers the rich dynamics of deformation in random flows, provides methods to characterize deformation from macroscopic observations, corrects classical fluid stretching models and calls for a reassessment of experimental data and fluid stretching models in turbulent and chaotic flows.

Fluid deformation underpins myriad fluid-borne processes including solute mixing, particle transport and deposition, chemical and biological reactions [1, 2]. Deformation can fundamentally augment these processes [3, 4] and the rate of deformation is critical to their comprehension and prediction in turbulent or chaotic flows. The basic deformation process – stretching of a material line – acts an input to many models [5, 6, 7] of these phenomena. Despite its fundamental role, line stretching in random flows is not fully understood, and for over half a century this process been quantified via phenomenological models [8, 9, 10, 11, 12] of classical fluid mechanics.

In this study we correct these models by performing an *ab initio* analysis of line stretching in random flows. This analysis uncovers the rich dynamics of line stretching under Fickian and non-Fickian transport, reconciles previously incompatible results, provides methods to characterize stretching from macroscopic measurements, and calls for a reconsideration of experimental data and models of fluid stretching and associated phenomena.

The two fundamental deformation measures are the Lyapunov exponent λ_∞ , which characterizes the asymptotic growth rate of infinitesimal line elements δl as

$$\lambda_\infty = \lim_{t \rightarrow \infty} \frac{1}{t} \ln \frac{\delta l(\mathbf{X}, t)}{\delta l(\mathbf{X}, 0)} = \lim_{t \rightarrow \infty} \frac{1}{2t} \ln \nu(\mathbf{X}, t), \quad (1)$$

and the topological entropy h which measures the growth rate of the length $l(t)$ of finite material lines as

$$h = \lim_{t \rightarrow \infty} \left(h(t) \equiv \frac{1}{t} \ln \frac{l(t)}{l(0)} \right), \quad (2)$$

where $h(t)$ is the finite-time topological entropy (FTLE). The advantage of h over λ_∞ is that it only requires measurement of macroscopic deformation (i.e. growth of $l(t)$), rather than microscopic stretching. For ergodic purely hyperbolic flows, there exists some de-

bate regarding these measures. Workers in ergodic theory [13, 14, 15, 16] prove these measures are equivalent

$$h = \lambda_\infty, \quad (3)$$

which corresponds to a temporal average of stretching rates. Conversely, fluid physicists [8, 9, 10, 11, 12] propose that fluid stretching follows a sequential process, leading to a log-normal distribution of $\ln \delta l(t)$ with mean $\lambda_\infty t$ and variance $\sigma_\lambda^2 t$ and the ensemble average

$$h = \lambda_\infty + \sigma_\lambda^2/2. \quad (4)$$

This discrepancy can be large, with $\sigma_\lambda^2 \gg \lambda_\infty$ in turbulent [17] and laminar [18] flows. In this study we reconcile this discrepancy, provide methods to estimate λ_∞ and σ_λ^2 from macroscopic $l(t)$ data and uncover the true dynamics of line stretching in random flows.

Fluid Deformation as a Random Walk. Fluid stretching is characterized by the fluid deformation gradient tensor $\mathbf{F}(\mathbf{X}, t) = \partial \mathbf{x} / \partial \mathbf{X}$ between the Eulerian \mathbf{x} and Lagrangian \mathbf{X} frames, which evolves according to the Lagrangian velocity gradient tensor $\boldsymbol{\epsilon}(\mathbf{X}, t) \equiv \nabla \mathbf{v}(\mathbf{x}(\mathbf{X}, t), t)^\top$ as $\dot{\mathbf{F}} = \boldsymbol{\epsilon} \cdot \mathbf{F}$, with $\mathbf{F}(\mathbf{X}, 0) = \mathbf{1}$. In the Protean coordinate frame \mathbf{x}' [19], both $\boldsymbol{\epsilon}'$ and \mathbf{F}' are upper triangular. For both steady and unsteady flows, the diagonal and off-diagonal elements of $\boldsymbol{\epsilon}'$ respectively correspond to principal stretches and shears. The element $\epsilon \equiv \epsilon'_{22}$ is associated with the largest Lyapunov exponent, with $\lambda_\infty = \langle \epsilon \rangle$. As F'_{22} bounds exponential growth of \mathbf{F}' and the largest eigenvalue $\nu(\mathbf{X}, t)$ of the Cauchy-Green tensor $\mathbf{C} \equiv \mathbf{F}' \cdot \mathbf{F}'^\top = \mathbf{F} \cdot \mathbf{F}^\top$, then δl grows as

$$\ln \delta l(\mathbf{X}, t) \approx \ln F'_{22}(\mathbf{X}, t) = \int_0^t dt' \epsilon(\mathbf{X}, t'). \quad (5)$$

Steady Flow. For steady flows, the velocity spatially decorrelates at distance $s = \ell_c$ along pathlines,

hence both $v = |\mathbf{v}|$ and ϵ follow a spatial Markov process [19, 20]. For such flows that exhibit spatial decorrelation (SD), the stretching increment $\xi \equiv \ln(\delta l)$ may be modelled via the continuous time random walk (CTRW)

$$\xi_{n+1} = \xi_n + \epsilon_n \tau_n, \quad t_{n+1} = t_n + \tau_n, \quad s_{n+1} = s_n + \ell_c, \quad (6)$$

where $\tau_n = \ell_c/v_n$ is the waiting time between increments. Typically the velocity PDF scales as $p_v(v) \sim v^{\beta-1}$ for $v \ll \langle v \rangle$, hence the waiting time distribution $\psi(\tau)$ scales as $\psi(\tau) \sim \tau^{-\beta-1}$ for $\tau \gg \langle \tau \rangle$ and the moments μ^q of $\psi(\tau)$ are finite for $q < \beta$. Fickian transport arises if $\beta > 2$, where the mean and variance of ψ are finite, and the CTRW (6) converges to the Brownian motion with drift

$$d\xi = \lambda_\infty dt + \sigma_\lambda dW(t), \quad (7)$$

where $W(t)$ is a Wiener process and $\sigma_\lambda^2 = \sigma_\epsilon^2/\gamma$ with $\gamma = \langle \tau^2 \rangle / \langle \tau \rangle$ for SD flows [18]. Conversely, non-Fickian (anomalous) transport arises if $1 < \beta < 2$, and the variance of ξ grows in time as $\sigma_\xi^2 \sim t^{3-\beta}$.

Unsteady Flow. Unsteady flows are denoted as spatio-temporal decorrelating (STD) flows as the Lagrangian velocity decorrelates in space and time. These flows are non-Markovian in time and space and can display strong intermittency in e.g. turbulent flow. Despite this intermittency, these velocities can be rendered Markovian with respect to a correlation variable r which is a function of the local velocity [21], leading to the CTRW

$$\xi_{n+1} = \xi_n + \epsilon_n \tau_n, \quad t_{n+1} = t_n + \tau_n, \quad s_{n+1} = s_n + l_n, \quad (8)$$

where $\tau_n = \ell_c/(v_n + \ell_c/\tau_c)$, $l_n = v_n \tau_n$ and ℓ_c and τ_c respectively are the correlation length and time of Lagrangian velocity fluctuations, also leading to the scaling $\psi(\tau) \sim \tau^{-\beta-1}$ for $\tau \gg \langle \tau \rangle$. This CTRW also converges to (7) for $\beta > 2$ with variance $\sigma_\lambda^2 = ??$ [22], and yields anomalous transport for $1 < \beta < 2$. Hence fluid stretching in SD and STD flows is governed by similar CTRW processes. We first consider Fickian line stretching before extending to the non-Fickian case.

Fluid Stretching is an Autocatalytic Process. The stretching of a finite sized material line \mathcal{L} of original length l_0 follows an *autocatalytic* process due to due to spatial decorrelation of $\epsilon(X(x), t)$ (with Eulerian x correlation length ℓ_c) along \mathcal{L} during stretching. Under this process, a finite line element of \mathcal{L} of length $\Delta l(t) < \ell_c$ undergoes correlated stretching until it exceeds ℓ_c , upon which it samples independent stretching rates ϵ and so is comprised of independent stretching regions which also stretch and decorrelate as the process continues.

A simple model that captures this process is one where \mathcal{L} is comprised of $N(t)$ line elements of length $\Delta l_i(t)$ with $i = 1 : N(t)$ and $\Delta l_i(t) \leq \ell_c$ which grow uniformly in

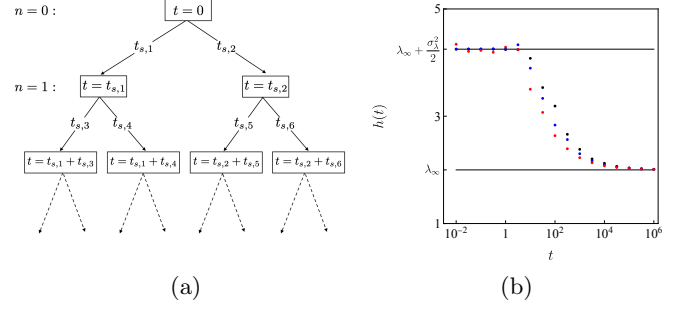


FIG. 1: (a) Schematic of the autocatalytic model for fluid stretching given by a binary tree, where the n -th generation (depicted by each horizontal level) of the tree contains $N(t) = 2^n$ members and the arrival time at each branch is given by the sum of stretching times t_s along the path from $t = 0$. (b) Evolution of finite-time topological entropy $h(t)$ computed from a log-normal distribution with log-mean $\lambda_\infty t$ and log-variance $\sigma_\lambda^2 t$ with $\lambda_\infty = 2$ and $\sigma_\lambda^2 = 9/2$ for various t and $N = 10^4$ (red dots), $N = 10^6$ (blue dots) and $N = 10^8$ (black dots) random variates, indicating transition from ensemble average $\lambda_\infty + \sigma_\lambda^2/2$ to temporal average λ_∞ with increasing t .

space with independent random stretching rates $\epsilon_i(t)$ as

$$l(t) = \sum_{i=1}^{N(t)} \Delta l_i(t) \quad \Delta l_i(t) = \exp(\xi_i(t)), \quad (9)$$

where $\xi_i(t)$ evolves as per (7). Elements of initial length $\Delta l(t_0) = \ell_c/2$ are stretched until they reach length $\Delta l(t_0 + \tau_s) = \ell_c$ after stretching time τ_s , at which time they break up into two new elements of length $\ell_c/2$ and the process continues. Hence $N(t)$ follows the autocatalytic process $A \rightarrow 2A$ as shown by the binary tree in Fig. 1(a), where $N(t) = 2^n$ at generation n of the tree.

The stretching time τ_s is given by the first passage time distribution of (7) for a particle with initial length $\Delta l(t_0) = \ell_c/2$ reaching $\Delta l(t_0 + t_s) = \ell_c$, the solution of which [23] yields an inverse Gaussian distribution for $\tau_s \geq 0$ with mean $\ln 2/\lambda_\infty$ and scale parameter $(\ln 2)^2/\sigma_\lambda^2$

$$\psi(\tau_s) = \frac{\ln 2}{\sqrt{2\pi\sigma_\lambda^2\tau_s^3}} \exp \left[-\frac{\lambda_\infty^2 \left(\tau_s - \frac{\ln 2}{\lambda_\infty} \right)^2}{2\sigma_\lambda^2\tau_s} \right]. \quad (10)$$

Hence [22] the conditional distribution $p_{t|n}(t|n)$ of the generation time t of each element at generation n converges with n to a Gaussian with mean $\langle t|n \rangle = n \ln 2/\lambda_\infty$ and variance $\sigma_t^2 = n \ln 2^2/\sigma_\lambda^2$, and so [22] the marginal distribution $p_{n|t}(n|t)$ of n at time t converges to a Gaussian distribution with mean and variance

$$\langle n|t \rangle = \frac{\lambda_\infty}{\ln 2} t, \quad \sigma_n^2 = \frac{\sigma_\lambda^2}{\ln 2^2} t. \quad (11)$$

As such, $\ln N(t)$ is Gaussian distributed with mean λ_∞ and variance σ_λ^2 , yielding [22] the ensemble average (4):

$$\langle N(t) \rangle = \int_{-\infty}^{\infty} dn 2^n p_{n|t}(n|t) = \exp \left[\left(\lambda_\infty + \frac{\sigma_\lambda^2}{2} \right) t \right]. \quad (12)$$

Fig. 1b shows that for numerical simulations [22] with fixed $N(t) = \text{const.}$, $h(t)$ converges to the temporal average (3), whereas under this autocatalytic model [22] with exponential growth of $N(t)$, $h(t)$ converges to the ensemble average (4). However line stretching involves further dynamics which must be accounted for.

Ensemble and Temporal Averaging. Evolution of \mathcal{L} also involves competition between ensemble and temporal averaging. The length $l(t)$ of \mathcal{L} grows as

$$l(t) = \int_0^{l_0} dX \delta l(X, t) = \int_0^{l_0} dX \exp(\lambda(X, t) t), \quad (13)$$

where $X \in [0, l_0]$ denotes the Lagrangian coordinate along \mathcal{L} , and the finite time Lyapunov exponent (FTLE) $\lambda(X; t) \equiv \frac{1}{t} \int_0^t dt' \epsilon(X; t')$ with fluctuation $\lambda'(X, t) \equiv \lambda(X, t) - \lambda_\infty$. Under the assumption that as \mathcal{L} is stretched it ergodically samples the entire ensemble of λ' ,

$$l(t) = l_0 \exp(\lambda_\infty t) \int_{-\infty}^{\infty} d\lambda' p_y(\lambda'|t) \exp(\lambda' t), \quad (14)$$

where the FTLE fluctuation distribution $p_y(y|t)$ is

$$p_y(y|t) \equiv \lim_{L \rightarrow \infty} \frac{1}{L} \int_0^L dX \delta[y - \lambda'(X, t)]. \quad (15)$$

From (7), $p_y(\lambda'|t)$ is Gaussian with zero mean and variance σ_λ^2/t , hence evaluation of (14) recovers (4) in the limit $t \rightarrow \infty$. However, we also note that the FTLE λ represents a temporal average which converges to λ_∞ as $t \rightarrow \infty$. Similarly, the FTLE fluctuation λ' converges to zero with time as $\langle \lambda'^2 \rangle = \sigma_\lambda^2/t$, and application [22] of this temporal average to (13) recovers (3).

Finite Sample Distribution. The competition between ensemble and temporal averaging during fluid stretching can be posed as a finite sampling process. To account for the finite number $N(t)$ of independent variates ξ_i expressed along \mathcal{L} , (14) can be expressed in terms of the finite sample distribution $p_{y,N}(\lambda'|t)$, defined as

$$p_{y,N}(y|t) \equiv \frac{1}{l_0} \int_0^{l_0} dX \delta[y - \lambda'(X, t)], \quad (16)$$

which converges to $p_y(\lambda'|t)$ as $N(t) \rightarrow \infty$. Note that while $p_{y,N}$ in (19) is defined in the Lagrangian frame X , the velocity gradient ϵ in (5) has correlation length ℓ_c in the Eulerian frame x , leading to spatial decorrelation of ϵ along \mathcal{L} and autocatalytic stretching. Equation (16) can be shown [22] to be consistent with the autocatalysis by transforming (16) to the Eulerian frame via

$$dX = \exp[-\lambda(X(x), t)t] dx, \quad x(t, \ell_0) = \ell(t) \quad (17)$$

to yield

$$p_{y,N}(y|t) = \frac{1}{l_0} \frac{\exp(-yt)}{\exp(\lambda_\infty t)} \int_0^{l(t)} dx \delta[y - \lambda'(X(x), t)]. \quad (18)$$

When combined with autocatalytic stretching model [22], the sample integral (18) recovers the Gaussian distribution $p_y(y|t)$ for $N(t) \rightarrow \infty$. For finite $N(t)$ the truncated Gaussian distribution is then

$$p_{y,N}(y|t) \equiv \begin{cases} \frac{\exp\left(-\frac{y^2}{2\sigma_y^2}\right)}{\sqrt{2\pi\sigma_y^2} \text{erf}\left(\frac{\lambda'_m}{\sqrt{2}\sigma_y}\right)} & \text{if } |y| < \lambda'_m(t), \\ 0 & \text{otherwise,} \end{cases} \quad (19)$$

where $\lambda'_m(t)$ is the limiting value of λ' due to finite sampling. $\lambda'_m(t)$ is related to $N(t)$ as

$$1 - \int_{-\lambda'_m(t)}^{\lambda'_m(t)} dy \frac{\exp\left(-\frac{y^2}{2\sigma_y^2}\right)}{\sqrt{2\pi\sigma_y^2}} = \frac{1}{N(t)}, \quad (20)$$

hence $\lambda'_m(t) = \sqrt{2} \sigma_y(t) \text{erf}^{-1}(1 - 1/N) = \sigma_y(t) A[N]$, where $A[N(t)] \approx \sqrt{2 \ln N(t)}$ as $N \rightarrow \infty$. From (19), (14) simplifies to

$$\frac{l(t)}{l_0} e^{-\lambda_\infty t} = \frac{\exp\left(\frac{\sigma_y^2(t) t^2}{2}\right)}{\sqrt{2\pi} \text{erf}\left(\frac{A[N(t)]}{\sqrt{2}}\right)} \int_{\sigma_y t - A}^{\sigma_y t + A} dy e^{-\frac{y^2}{2}}, \quad (21)$$

which shows that $N(t)$ governs convergence of $h(t)$.

Temporal Decorrelation. The competition between ensemble- and temporal-dominated averaging can be quantified by considering that under Fickian transport, the CTRWs (6) and (8) correspond to a velocity gradient fluctuation $\epsilon' \equiv \epsilon - \lambda_\infty$ that decorrelates temporally as

$$\langle \epsilon'(t) \epsilon'(t') \rangle = \sigma_\lambda^2 \gamma \exp(-\gamma |t - t'|), \quad (22)$$

where $\gamma = 1/\tau_v$ for SD flows and $\gamma = ?$ for STD flows. From (22), the variance of $\lambda'(X, t)$ evolves as

$$\begin{aligned} \sigma_y^2(t) &\equiv \langle \lambda'(X, t)^2 \rangle = \frac{1}{t^2} \int_0^t dt' \int_0^t dt'' \langle \epsilon'(t') \epsilon'(t'') \rangle \\ &= \frac{\sigma_\lambda^2 \gamma}{(\gamma t)^2} [\gamma t - 1 + \exp(-\gamma t)], \end{aligned} \quad (23)$$

which for small times $\gamma t \ll 1$ yields $\sigma_y^2(t) = \sigma_\lambda^2 \gamma / 2$, and for long times $\gamma t \gg 1$ yields $\sigma_y^2(t) = \sigma_\lambda^2 / t$.

Small Time Dynamics. For small times $\gamma t \ll 1$, the integration limits in (21) approximate as $\sigma_\lambda t / \gamma \pm A[N(0)]$, and for $t \ll A[N(0)]\gamma / \sigma_\lambda$, $\sigma_y(t)t \pm A[N(t)] \approx \pm A[N(t)]$, hence [22] $l(t)$ then grows with time as

$$l(t) = l_0 \exp(\lambda_\infty t + \sigma_\lambda^2 t / 2), \quad (24)$$

and so for $\gamma t \ll 1$, $h(t)$ converges to (4).

Long Time Dynamics. If $N(t)$ grows sub-exponentially with time, then for long times $\gamma t \gg 1$ with $\sigma_\lambda \sqrt{t} > A[N(t)] \approx \sqrt{\ln N(t)}$, and (21) evaluates [22] to

$$h(t) = \lambda_\infty + \frac{1}{t} \ln \left(\sigma_\lambda \sqrt{t \ln N(t)} - \frac{\ln N(t)}{2} \right), \quad (25)$$

which converges to the temporal average (3). Conversely, if $N(t)$ grows exponentially with time such that $\sigma_\lambda \sqrt{t} \lesssim A[N(t)] \approx \sqrt{\ln N(t)}$, (21) evaluates to [22]

$$h = \lambda_\infty + \frac{\sigma_\lambda^2}{2} - f(\lambda_\infty, \sigma_\lambda^2), \quad (26)$$

where $0 \leq f \leq h$ is a correction to the ensemble average (4) which is zero for $\sigma_\lambda^2 \geq \lambda_\infty$.

Convergence of $h(t)$. Equations (24)-(26) constitute the first major results of this paper. At short times $\gamma t \ll 1$, $h(t)$ converges to (4), which explains why it is consistently observed in experimental [24] and computational studies. However, at long times $\gamma t \gg 1$, convergence of h is controlled by the relative convergence of $\sigma_\lambda / \sqrt{t}$ to the temporal average (3) and $\sqrt{\ln N(t)} / t$ to the ensemble average (4). These dynamics are reflected in Fig. 1a, which shows the evolution of $h(t)$ for $N(t) = \text{const.}$ and $N(t) \sim \exp(t)$ iid Gaussian variates with $\lambda_\infty = 1$, $\sigma_\lambda^2 = 2$. As expected, at short times, both set of variates return the ensemble average (4), but at long times the case $N(t) = \text{const.}$ converges to (3) due to temporal averaging, whereas the ensemble average (4) is sustained for $N(t) \sim \exp(t)$. Hence line stretching in random flow depends intimately upon the dynamics of $N(t)$, which we examine as follows.

Line Stretching, Folding and Dispersion. It appears reasonable to assume $N(t) \approx l(t) / \ell_c$, leading to exponential growth of $N(t)$. However, while neighboring variates ξ_i along \mathcal{L} may be independent, the ensemble $\{\xi_i\}$ may not consist of independent variates due to folding of \mathcal{L} , yielding fractal line distributions such as that shown in Fig. 1c which may be characterized in terms of fractal dimension $1 < d_f < d$ in a d -dimensional flow [25].

Coarse-graining \mathcal{L} over the correlation length ℓ_c yields a well-defined evolving finite support region $\Omega(t)$ with

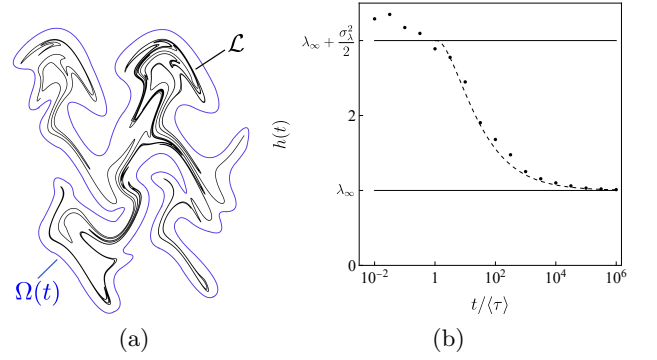


FIG. 2: (a) Folding of a stretched and folded material line \mathcal{L} (black line, generated from a time-periodic sine flow) over a coarse-grained finite support region $\Omega(t)$ (bounded by the blue line). (b) Convergence of finite-time topological entropy $h(t)$ (black dots) via statistical simulation of the steady CTRW (6) with $N(t) = 80t$ particles from ensemble average $\lambda_\infty + \sigma_\lambda^2/2 = 3$ to the temporal average $\lambda_\infty = 1$ due to finite sampling along \mathcal{L} . Dashed line indicates theoretical convergence of $h(t)$ to λ_∞ given by (25).

volume $V_\Omega(t)$. As the ensemble $\{\xi_i\}$ is drawn from $\Omega(t)$, the number of independent variates $N(t) = V_\Omega(t) / \ell_c^d$. Only in the absence of folding (where $d_f = 1$ and $V_\omega = \ell_c^{d-1} l(t)$) is $N(t) \propto l(t)$. The simplest model for $V_\Omega(t)$ corresponds to an isotropic dispersion process, where $N(t)$ grows as

$$N(t) \approx (2D_\infty t)^{d/2} \ell_c^{-d}, \quad (27)$$

and D_∞ is the asymptotic dispersivity of the material line due to pure advection. Although line dispersion dynamics may vary with flow type, leading to different scalings than (27), all SD and STD flows exhibit algebraic growth of $V_\Omega(t)$ due to line folding, hence $N(t)$ is always sub-exponential, so from (25), so temporal averaging (4) dominates as $h(t) \rightarrow h = \lambda_\infty$. Convergence of $h(t)$ at short (24) and long (25) times means that λ_∞ and σ_λ^2 can be easily estimated from macroscopic line stretching data $l(t)$ in Fickian flows without need for measurement of small scale stretching rates.

Line Stretching Under Anomalous Transport. We now consider the case of non-Fickian (anomalous) transport. For simplicity of exposition, we consider the CTRW (6) for steady flow, with the understanding that unsteady flow only differs in σ_λ^2 . For $1 < \beta < 2$, the mean stretching increment $\langle \xi \rangle = \langle \lambda \rangle t = \lambda_\infty t$ and variance $\langle \xi^2 \rangle$ from the Lévy walk (6) scales in the long time limit as [26, 27] $\langle \xi^2 \rangle = \sigma_\lambda^2 t^{3-\beta}$ with $\sigma_\lambda^2 = ?$, whereas for unsteady flow $\sigma_\lambda^2 = ?$. Similarly, the FTLE variance converges with time as

$$\langle \lambda'^2 \rangle = \sigma_y^2(t) = \sigma_\lambda^2 t^{1-\beta}. \quad (28)$$

Rebenshtok *et al.* [27] shows that for the Lévy walk (6)

with $\gamma t \gg 1$, the distribution of ξ converges to

$$\lim_{t \rightarrow \infty} p_{\xi'}(\xi'|t) = t^{-\beta} \mathcal{I}\left(\frac{\xi'}{t}\right), \quad (29)$$

where \mathcal{I} is the infinite density $\mathcal{I}(\bar{\epsilon})$ and $\bar{\epsilon} \equiv \langle \xi' \rangle / t$. On physical grounds the velocity gradient is everywhere finite, hence $p_{\epsilon}(\epsilon)$ is bounded. For simplicity of exposition we consider a uniform distribution for $p_{\epsilon}(\epsilon) \sim U[\lambda_{\infty} - a, \lambda_{\infty} + a]$ centered about λ_{∞} with variance $\sigma_{\lambda}^2 = 3a$, and note that other bounded distributions generate similar results [22]. For uniform $p_{\epsilon}(\epsilon)$ we find [22]

$$\mathcal{I}(|\bar{\epsilon}|) = \frac{B}{2a} \left[\frac{\beta}{\beta+1} \left(\frac{a^{\beta+1}}{|\bar{\epsilon}|^{\beta+1}} - 1 \right) - \frac{\beta-1}{\beta} \left(\frac{a^{\beta}}{|\bar{\epsilon}|^{\beta}} - 1 \right) \right], \quad (30)$$

where $|\bar{\epsilon}| < a$. As shown in Fig. 3a, at finite times $p_{\xi'}(\xi'|t)$ is described by a finite Levy-stable distribution about $\xi' = 0$ (see [22] for details), but converges toward $\mathcal{I}(|\bar{\epsilon}|)$ as $t \rightarrow \infty$ which is singular about $\bar{\epsilon} = 0$. This convergence is analogous to convergence of $p_y(y|t) \rightarrow \delta(y)$ in the Fickian case, and corresponds to convergence of $h(t)$ to the temporal average.

Similar to the Fickian case, growth of $l(t)$ is characterized by the finite sample PDF $p'_{\xi,N} \propto p_{\xi'} \mathbb{I}(-\lambda'_m(t)t < \xi < \lambda'_m(t)t)$ where $\lambda'_m(t)$ is the limiting value of $|\lambda'|$ due to finite sampling along \mathcal{L} , and

$$\frac{l(t)}{l_0} \exp(-\lambda_{\infty} t) = \int_{-\infty}^{\infty} d\xi' p_{\xi',N}(\xi'|t) e^{\xi'}. \quad (31)$$

Following (20), the truncation value $\lambda'_m(t)$ is

$$2 \int_{\lambda'_m(t)}^a dy t^{1-\beta} \mathcal{I}(y) = \frac{1}{N(t)}, \quad (32)$$

which, to leading order around $\lambda'_m = a$ [22] is

$$\frac{B t^{1-\beta}}{2} \left(1 - \frac{\lambda'_m(t)}{a} \right)^2 \approx \frac{1}{N(t)}. \quad (33)$$

For large t the integral (31) is dominated by behavior near the upper tail $y = a$, and so to leading order

$$\frac{l(t)}{l_0} \exp(-\lambda_{\infty} t) \approx \int_{y_c(t)}^{\lambda'_m(t)} dy t^{1-\beta} \mathcal{I}(y) \exp(yt), \quad (34)$$

where $0 < y_c(t) < a$ is the y -value associated with the crossover of $p_{y,N}(y|t)$ from the infinite density \mathcal{I} to the central Levy stable distribution. To leading order, evaluation [22] of (34) scales with t as $t^{-1-\beta} \exp(\lambda'_m(t)t)$, hence from (34) the material line length evolves as

$$l(t) \sim l_0 t^{-1-\beta} \exp([\lambda_{\infty} + \lambda'_m(t)]t) \quad (35)$$

and so the finite time topological entropy is then

$$h(t) = \lambda_{\infty} + \frac{\sigma_{\lambda}^2}{3} \left(1 - \sqrt{\frac{2 t^{\beta-1}}{B N(t)}} \right), \quad (36)$$

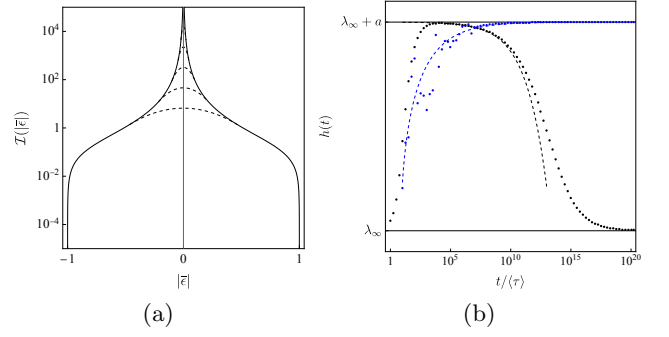


FIG. 3: (a) Solid line: Infinite density $\mathcal{I}(|\epsilon|)$ from (30) for $a = 1$, $B = 1$, $\beta = 3/2$. Dashed lines represent Levy-stable part [22] of finite time PDF $p_{\xi'}(\xi'|t)$ for $t/\tau = 10, 10^2, 10^3, 10^4, 10^5$. (b) Convergence of finite time topological entropy $h(t)$ to $h = \lambda_{\infty} + a$ for (blue dots) statistical simulation of (6) and (dashed blue line) from (36) with $N(t) = t$ particles. Evolution of $h(t)$ from (black dots) statistical simulation and (black dashed line) theoretical evolution of $h(t)$ from (36) with $N(t) = 10^7$ particles.

which converges to $h = \lambda_{\infty} + \sigma_{\lambda}^2/3$ for $N(t) \gtrsim t^{\beta-1}$ as $t \rightarrow \infty$. As $N(t) \sim t^{d/2}$ with $d \geq 2$ and $1 < \beta < 2$, this is always fulfilled, hence the ensemble average (4) dominates for anomalous transport.

Figure 3b shows that for linearly growing $N(t)$ (which corresponds to e.g. dispersion in a 2D flow), the finite time topological entropy converges to $\lambda_{\infty} + \sigma_{\lambda}^2/3$ as the growth of $N(t)$ in (36) dominates over convergence toward the core of the infinite density PDF $\mathcal{I}(|\bar{\epsilon}|)$ (which scales as $t^{\beta-1}$). Conversely, for fixed $N(t)$, Figure 3b shows that $h(t)$ slowly converges to λ_{∞} at long times as given by (36).

Closing Remarks. Hence line stretching in anomalous (non-Fickian) flows is fundamentally different to that of Fickian systems, where the algebraic growth of $N(t) \sim t^{d/2}$ due to line dispersion is sufficient to always dominate over growth of the singularity in p'_{ξ} at $\xi' = 0$ as $t^{\beta-1}$, leading to convergence to the ensemble average $h = \lambda_{\infty} + \sigma_{\lambda}^2/3$ as $t \rightarrow \infty$. Conversely, algebraic growth of $N(t)$ in Fickian flows is always dominated by convergence due to shrinking variance of the stretching distribution (which has Gaussian-tailed), leading to convergence to the temporal average $h = \lambda_{\infty}$ as $t \rightarrow \infty$. These results can also be extended to other flow classes. For flows which are random in time but have limited spatial variation, temporal averaging dominates as the growth of $N(t)$ is also limited. In general, for all Fickian purely hyperbolic non-random flows (which are thus chaotic and ergodic), temporal averaging is expected to dominate as $N(t)$ is sub-exponential due to folding. The extent to which this extends to the non-Fickian counterpart is a topic of future research. These *ab initio* results correctly resolve the dynamics of fluid deformation in Fickian and non-Fickian random flows. They generate provide methods to characterize stretching metrics

solely from $l(t)$ data, reconcile previously incompatible results and call for reconsideration of experimental data and models of fluid stirring, mixing, transport and reaction.

* Electronic address: daniel.lester@rmit.edu.au

- [1] P. E. Dimotakis, Annual Review of Fluid Mechanics **37**, 329 (2005).
- [2] P. A. Libby and F. A. Williams, Annual Review of Fluid Mechanics **8**, 351 (1976).
- [3] H. Aref, J. R. Blake, M. Budišić, S. S. Cardoso, J. H. Cartwright, H. J. Clercx, K. El Omari, U. Feudel, R. Golestanian, E. Guillard, *et al.*, Reviews of Modern Physics **89**, 025007 (2017).
- [4] K. R. Sreenivasan, Proceedings of the National Academy of Sciences **116**, 18175 (2019).
- [5] E. Villermaux and J. Duplat, Phys. Rev. Lett. **91**, 184501 (2003).
- [6] T. Tél, A. de Moura, C. Grebogi, and G. Károlyi, Physics Reports **413**, 91 (2005).
- [7] G. Haller and T. Sapsis, Physica D: Nonlinear Phenomena **237**, 573 (2008).
- [8] W. J. Cocke, The Physics of Fluids **12**, 2488 (1969).
- [9] S. S. Girimaji and S. B. Pope, Journal of Fluid Mechanics **220**, 427 (1990).
- [10] J. Duplat, C. Innocenti, and E. Villermaux, Phys. Fluids **22**, 035104 (2010).
- [11] J. Kalda, Phys. Rev. Lett. **84**, 471 (2000).
- [12] E. Villermaux, Annu. Rev. Fluid Mech. **51**, 245 (2019).
- [13] S. E. Newhouse, Ergodic Theory and Dynamical Systems **8**, 283 (1988).
- [14] S. Newhouse and T. Pignataro, Journal of Statistical Physics **72**, 1331 (1993).
- [15] C. Matsuoka and K. Hiraide, Chaos: An Interdisciplinary Journal of Nonlinear Science **25**, 103110 (2015).
- [16] Y. Yomdin, Israel Journal of Mathematics **57**, 285 (1987).
- [17] G. A. Voth, G. Haller, and J. P. Gollub, Phys. Rev. Lett. **88**, 254501 (2002).
- [18] D. R. Lester, M. Trefy, G. Metcalfe, and M. Dentz, Journal of Fluid Mechanics (2024).
- [19] D. R. Lester, M. Dentz, T. L. Borgne, and F. P. J. D. Barros, Journal of Fluid Mechanics **855**, 770 (2018).
- [20] T. Le Borgne, M. Dentz, and J. Carrera, Phys. Rev. Lett. **101**, 090601 (2008).
- [21] M. Dentz and D. R. Lester, Journal of Fluid Mechanics (2025).
- [22] “Supplementary material,” .
- [23] R. Bhattacharya and E. C. Waymire, “First passage time distributions for Brownian motion with drift and a local limit theorem,” in *Random Walk, Brownian Motion, and Martingales* (Springer International Publishing, Cham, 2021) pp. 191–198.
- [24] M. Souzy, H. Lhuissier, Y. Méheust, T. Le Borgne, and B. Metzger, J. Fluid Mech **891** (2020).
- [25] E. Villermaux and Y. Gagne, Phys. Rev. Lett. **73**, 252 (1994).
- [26] M. Dentz, T. Le Borgne, D. R. Lester, and F. P. J. de Barros, Phys. Rev. E **92**, 032128 (2015).
- [27] A. Rebenshtok, S. Denisov, P. Hänggi, and E. Barkai, Phys. Rev. Lett. **112**, 110601 (2014).